Mass Profiles of Clusters at Large Radii from Weak Gravitational Lensing

D. Clowe [1], P. Schneider [1]
[1] *IAEF, Universität Bonn, Auf dem Hügel 71, 53121 Bonn, Germany*

Abstract. We present the weak lensing mass reconstructions of three clusters of galaxies from data taken on the ESO Wide Field Imager. We detect a lensing signal in all three clusters over a range of $1' < r < 17'$ ($\approx 0.1h^{-1}$Mpc $<$ r $<$ 2h^{-1}Mpc). We measure the best fitting SIS and NFW profiles for each cluster and show that in two of the three clusters the NFW profile is preferred to the SIS with marginal significance ($\sim 2\sigma$).

arXiv:astro-ph/0109260v1 17 Sep 2001

1 Introduction

In the past few years, high-resolution N-body simulations have been used to make predictions of the shapes of mass profiles for clusters of galaxies (e.g. [1], hereafter NFW). These profiles are characterized with a shallower, although still singular, core ($\rho \propto r^{-1}$ inside 100 kpc for NFW) than the classical singular isothermal sphere (SIS), but a steeper profile at large radii ($\rho \propto r^{-3}$ outside 1 Mpc). While the deviation at small radii is currently being investigated with X-ray and strong gravitational lensing studies (e.g. [2]), a perhaps more promising method to distinguish which of the profile classes is correct is measuring the mass profiles of the clusters at large radii with weak gravitational lensing.

Weak lensing is a study in which one measures the ellipticities of background galaxies and looks for a statistical deviation from an isotropic ellipticity distribution. This has the advantages over other methods to measure cluster masses that one gets a direct measure of the mass with no assumptions regarding they dynamical state of the cluster, and that, with current technology, the maximum radius at which one can measure the signal is limited primarily by the size of the detectors. To date most weak lensing cluster observations are limited to the central h^{-1} Mpc (e.g. [6]), but with the advent of large mosaic CCD cameras, we can now measure a weak lensing signal in half-degree fields with relatively little telescope time.

2 Observations and Data Reduction

We observed the clusters A1689 ($z = 0.182$), A1835 ($z = 0.252$), A2204 ($z = 0.152$), and A1347 on the nights of May 29 and 30, 2000 using the Wide Field Imager at the ESO/MPG 2.2m on La Silla. Each cluster was observed with 12 900s exposures in the R-band, which resulted in coadded images of $\sim 35' \times 34'$, with $\sim 87\%$ of each image having the full 3 hours of integration, and the remaining 13% having some smaller amount as the region was out of the field of view or between the gaps in the chip mosaic during some of the exposures. The final images have a FWHM of bright but unsaturated stars of $\sim 0\farcs7$. Object counts at a 3σ detection limit in the regions containing the full exposure time are complete to $R = 24.9$ for $2''$ radius aperture magnitudes, as measured by the point where the number counts depart from a power law.

Objects were detected and had their sizes, magnitudes, and second moments of the surface brightness measured using the IMCAT software package written by Nick Kaiser. Ellipticities were created from the measured second moments and were corrected for PSF anisotropy and circular smearing using the KSB techniques [4]. The corrected ellipticities can then be used as a direct estimator of the reduced shear, g, at the location of the galaxy. A1347 appears to consist of several small, unrelated groups of galaxies and stars clusters, and as such was used as a blank field to test that the observed weak lensing signals are in fact caused by the mass of the clusters and not by camera or telescope distortions.

The resulting cluster shears were then analyzed with two methods. The first method was using an inversion algorithm which uses the fact that both the shear and the mass surface density are second derivates of the surface potential to create a two dimensional image of the mass [5]. This surface

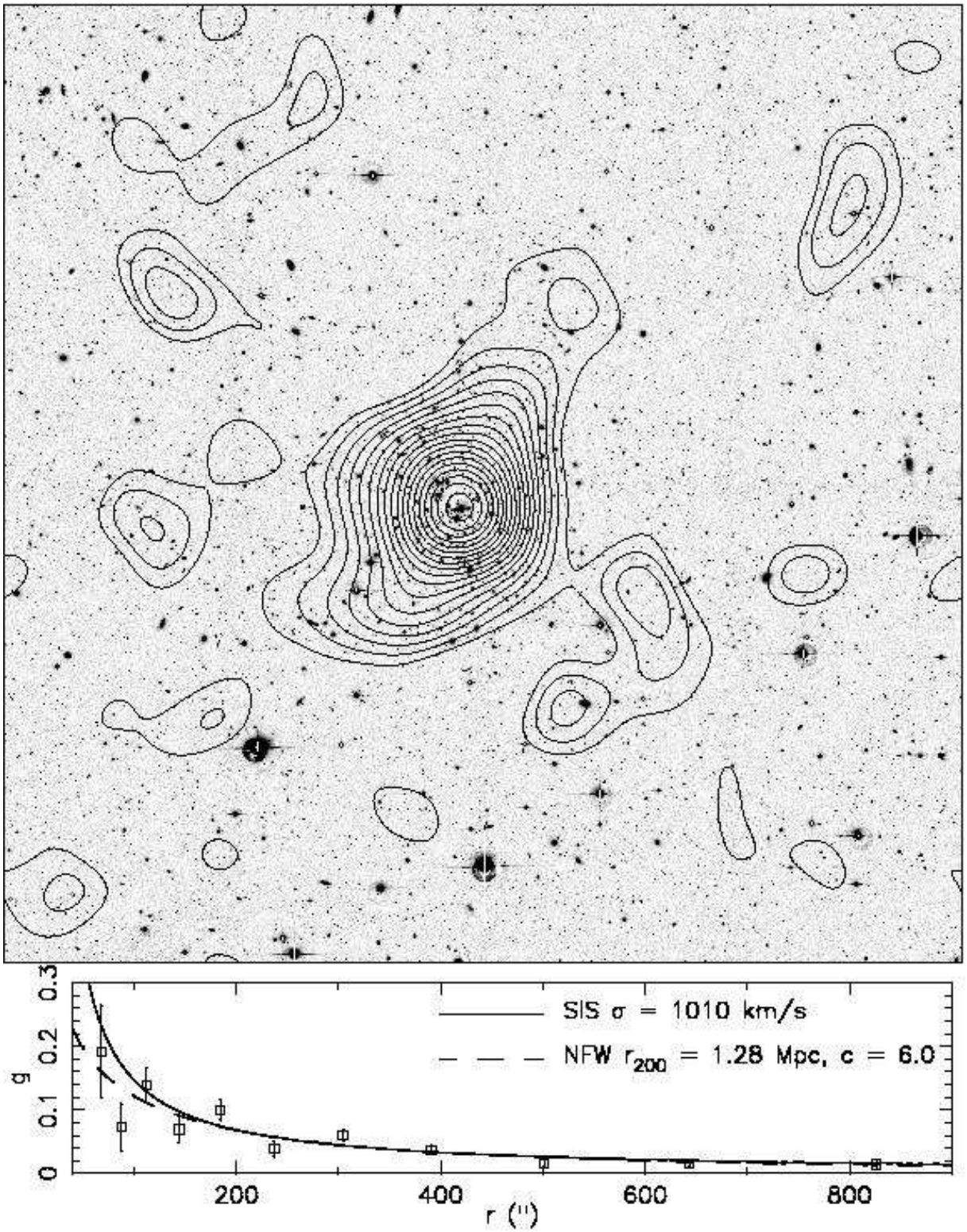

Figure 1: Shown above is the WFI R-band image of A1689 ($32\farcm8$, $\sim 4.28h^{-1}$Mpc, on a side) with the weak lensing mass reconstruction overlayed in contours. The mass reconstruction has been smoothed by a $1\farcm15$ Gaussian and each contour represents a change in κ of 0.01 above the mean at the edge of the image. Plotted below the image is the azimuthally averaged reduced shear profile, centered on the brightest cluster galaxy, in logarithmically spaced bins in radius. Also plotted are the best fitting SIS and NFW profiles. No correction factors have been made for the presence of foreground and cluster dwarf galaxies and faint stars in the background galaxy sample used to measure the shear. Correcting for this would increase the mass of the best fit models by 20-30% [3].

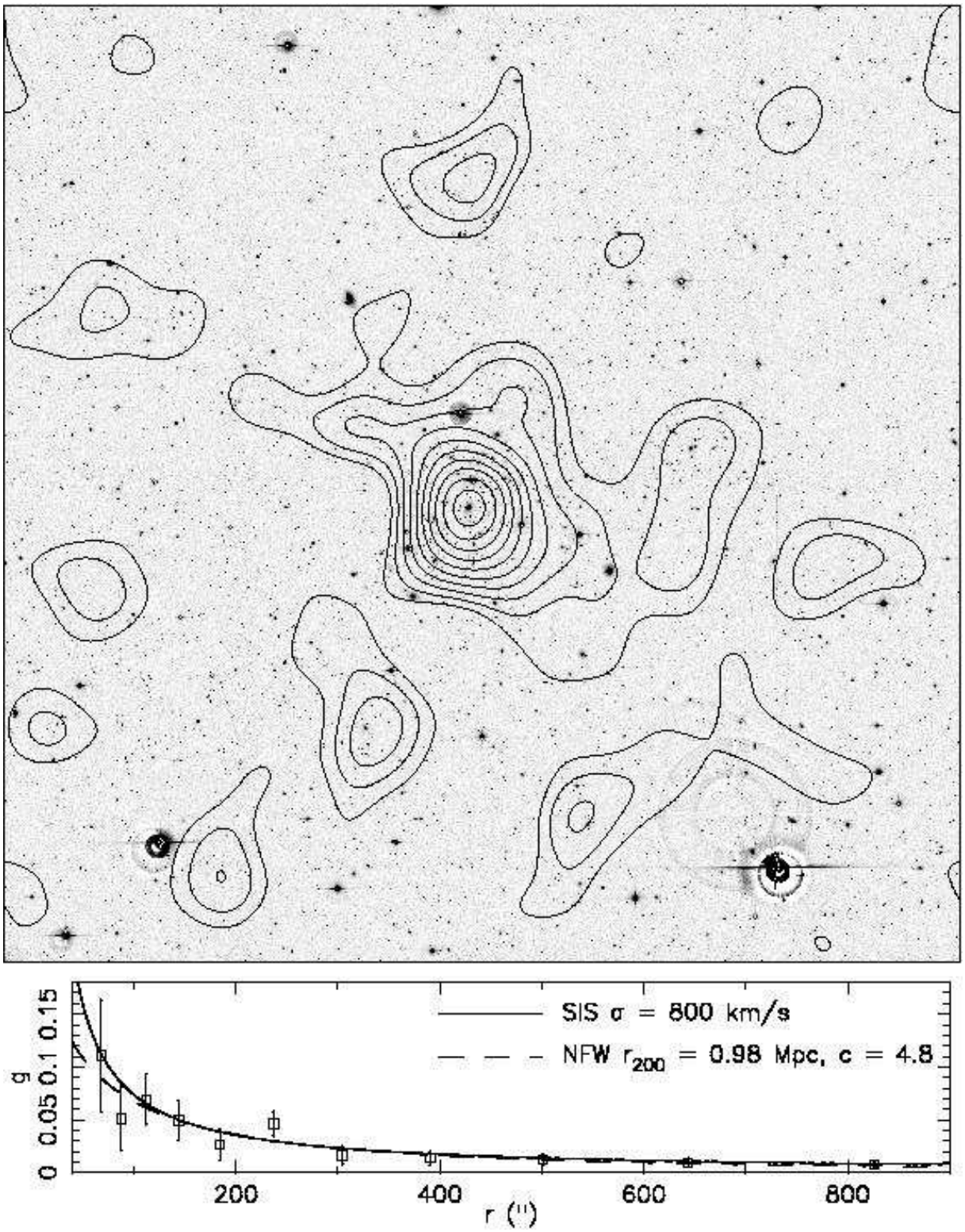

Figure 2: Shown above is the WFI R-band image of A1835 ($32\farcm8$, $\sim 5.42h^{-1}$Mpc, on a side) with the weak lensing mass reconstruction overlayed in contours. The mass reconstruction has been smoothed by a $1\farcm15$ Gaussian and each contour represents a change in κ of 0.01 above the mean at the edge of the image. Plotted below the image is the azimuthally averaged reduced shear profile, centered on the brightest cluster galaxy, in logarithmically spaced bins in radius. Also plotted are the best fitting SIS and NFW profiles. No correction factors have been made for the presence of foreground and cluster dwarf galaxies and faint stars in the background galaxy sample used to measure the shear. Correcting for this would increase the mass of the best fit models by 20-30%.

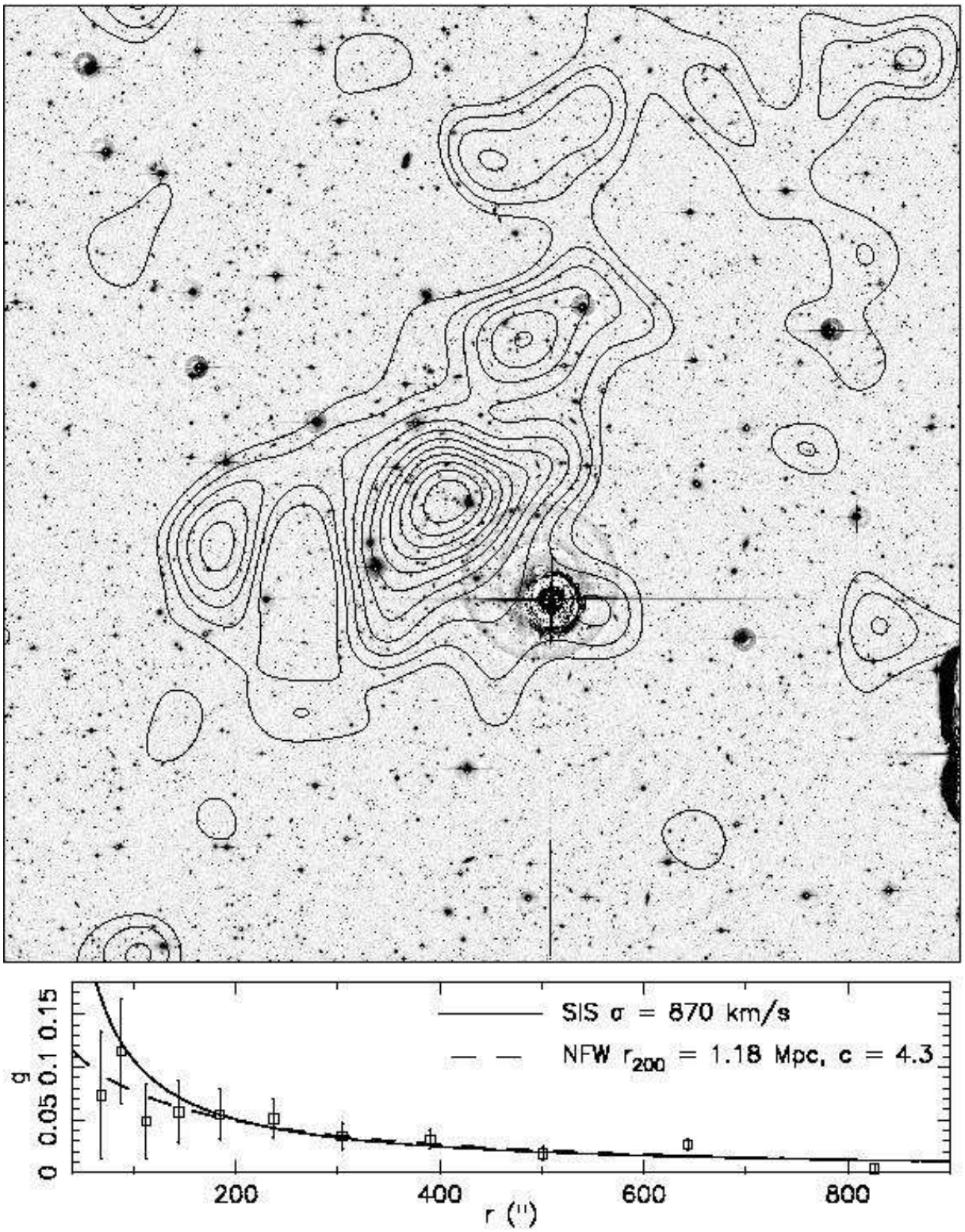

Figure 3: Shown above is the WFI R-band image of A2204 ($32\farcm8$, $\sim 3.63h^{-1}$Mpc, on a side) with the weak lensing mass reconstruction overlayed in contours. The mass reconstruction has been smoothed by a $1\farcm15$ Gaussian and each contour represents a change in κ of 0.01 above the mean at the edge of the image. Plotted below the image is the azimuthally averaged reduced shear profile, centered on the brightest cluster galaxy, in logarithmically spaced bins in radius. Also plotted are the best fitting SIS and NFW profiles. No correction factors have been made for the presence of foreground and cluster dwarf galaxies and faint stars in the background galaxy sample used to measure the shear. Correcting for this would increase the mass of the best fit models by 20-50%.

Table 1: best fit mass models

Cluster	SIS model			NFW model				F-test	
	σ (km/s)	$\chi^2/274$	S/N	r_{200} (Mpc)	c	$\chi^2/273$	S/N	F	Prob.
A1689	1030	0.921	13.7σ	1.28	6.0	0.910	13.6σ	4.18	96%
A1835	800	1.095	7.9σ	0.98	4.8	1.097	7.7σ	0.46	50%
A2204	870	1.060	8.1σ	1.18	4.3	1.049	8.0σ	3.54	94%

density distribution, however, can only be determined to within an unknown additive constant. The second method bins the shear radially around a chosen center of mass, the brightest cluster galaxy in this case. The resulting shear profile can then be fit with various mass profiles. The results for both techniques are shown for A1689, A1835, and A2204 in Figures 1, 2, and 3 respectively.

3 Discussion

As can be seen in the figures, all three clusters are detected at high signal-to-noise and the shear in the outermost bin is detected at greater than 3σ in A1689 and A1835, and greater than 3σ for the sum of the two outmost bins in A2204. The best fit mass models and their significances are given in table 1. All of the clusters have the center of the highest mass peak spatially coincident, to within the errors in the reconstruction, with the position of the brightest cluster galaxy, and all significant mass peaks have a corresponding peak in the galaxy distribution. Because the fields have been studied only in a single color, we do not have any information regarding which of the additional peaks are substructure within the cluster and which are foreground or background mass peaks. As such, while there appear to be filamentary structures extending from all three clusters in both the mass reconstructions and galaxy distributions, we cannot be sure that this is a detection of mass flowing into the cluster.

Also shown in table 1 are the best fit SIS and NFW models to the radial shear profiles of the clusters. While all three clusters are well fit by both profiles, as determined by the reduced χ^2, an F-test of an additional term, used to compare χ^2 values with different degrees of freedom, gives that the NFW profile is preferred over the SIS profile in A1689 and A2204 with 96% and 94% confidence. All of the cluster mass models, however, are much less massive than those predicted from the X-ray observations of the clusters [3][2],[7]. This is at least partially due to having only a single passband to use to select the background galaxy catalog. As a result, the catalog of objects with $23 < R < 25.5$ used in the mass reconstructions, which we assumed were only background galaxies ($z_{\rm bg} \sim 1$), is contaminated with faint stars and foreground and cluster dwarf galaxies. Estimates of the degree of contamination from other fields at similar galactic latitudes predict that 10-20% of the objects are faint stars, and a similar amount are (primarily cluster) dwarf galaxies. Thus, to correct for this contamination, the shear measurements and masses of the best fit models would need to be increased by ∼20-50%. Observation of these fields in additional passbands will allow for the selection of background galaxies by color, which should greatly reduce the level of foreground contamination.

References

[3] Clowe, D., Scheider, P., 2001, A&A, in press

[6] Clowe, D., Luppino, G. A., Kaiser, N., Gioia, I. M., 2000, ApJ, 539, 540

[7] Ebeling, H., Edge, A. C., Bohringer, H., et al. 1998, MNRAS, 301, 881

[4] Kaiser, N., Squires, G., Broadhurst, T., 1995, ApJ, 449, 460

[5] Kaiser, N., Squires, G., 1993, ApJ, 404, 441

[1] Navarro, J. F., Frenk, C. S., White, S. D. M., 1997, ApJ, 490, 493

[2] Schmidt, R. W., Allen, S. W., Fabian, A. C., 2001, MNRAS, submitted